DESIGN AND SIMULATION OF METAMATERIAL UNDER THE THZ FREQUENCY FOR SHORT-RANGE WIRELESS COMMUNICATION

A DISSERTATION

SUBMITTED IN PARTIAL FULFILMENT OF THE REQUIREMENTS FOR THE AWARD OF THE DEGREE OF

MASTER OF SCIENCE
IN
APPLIED PHYSICS

Submitted by:
Meenakshi (2K20/MSCPHY/12)
Prashant (2K20/MSCPHY/21)

Under the Supervisor of

Dr. Yogita Kalra

Dr. Kamal Kishor
Assistant Professor
Department of Applied Physics

DEPARTMENT OF APPLIED PHYSICS
DELHI TECHNOLOGICAL UNIVERSITY, DELHI
(Formerly Delhi College of Engineering)
Bawana Road, Delhi-110042

MAY,2022

CANDIDATE'S DECLARATION

We Meenakshi (2K20/MSCPHY/12) and Prashant (2K20/MSCPHY/21) of M.Sc. Applied physics hereby declares that Project dissertation **"Design and study of Metamaterial"** which is submitted by us to the Department of Applied Physics, **Delhi Technological University, Delhi** in partial fulfillment of the requirement for the award of the degree of Master of Science are original and not copied from any source without proper citation. This work has not previously formed the basis for the award of any degree, Diploma Associateship, Fellowship, or other similar title or recognition.

Meenakshi (2K20/MSCPHY/12)

Prashant (2K20/MSCPHY/21)
Place Delhi
Date: 10/05/2022

Conference: ICMPC **(**Publishing in Material Today Proceeding**)**

Submitted on: 31th March, 2022

Accepted on: 09th April, 2022

CERTIFICATE

This is to certify that the report entitled **"DESIGN AND STUDY OF METAMATERIAL"** submitted to the *Department of Applied Physics*, Delhi Technological University, Delhi in fulfilment of the requirement for the award of the Degree of Master of Science in Physics is a record of original research work done by **Meenakshi (2K20/MSCPHY/12) and Prashant (2K20/MSCPHY/21)** under our guidance. To the best of my knowledge, the above work has not been submitted in part or full for any Degree or Diploma to this University or elsewhere. I further certify that the publication and indexing information given by the student is correct.

Project Supervisor
Dr. Kamal Kishor

Assistant Professor
Department of Applied Physics
Delhi Technological University
Delhi- 110042

Project Supervisor
Dr. Yogita Kalra

Assistant Professor
Department of Applied Physics
Delhi Technological University
Delhi- 110042

Place Delhi

Date: 10/05/2022

turnitin **Similarity Report ID:** oid:27535:17016961

PAPER NAME

Final Dissertation (1)Report (2).docx

WORD COUNT	CHARACTER COUNT
4301 Words	**23105 Characters**
PAGE COUNT	FILE SIZE
21 Pages	**2.3MB**
SUBMISSION DATE	REPORT DATE
May 10, 2022 5:59 PM GMT+5:30	**May 10, 2022 5:59 PM GMT+5:30**

9% Overall Similarity

The combined total of all matches, including overlapping sources, for each database.

- 5% Internet database
- 5% Publications database
- Crossref database
- Crossref Posted Content database
- 5% Submitted Works database

Excluded from Similarity Report

- Bibliographic material
- Quoted material
- Small Matches (Less then 10 words)
- Manually excluded sources
- Manually excluded text blocks

turnitin

Similarity Report ID: oid:27535:17016961

9% Overall Similarity

Top sources found in the following databases:

- 5% Internet database
- Crossref database
- 5% Submitted Works database
- 5% Publications database
- Crossref Posted Content database

TOP SOURCES

The sources with the highest number of matches within the submission. Overlapping sources will not be displayed.

1	**Swinburne University of Technology on 2020-06-08** Submitted works	<1%
2	**tutorialspoint.com** Internet	<1%
3	**intechopen.com** Internet	<1%
4	**Bangladesh University of Professionals on 2022-02-08** Submitted works	<1%
5	**iopscience.iop.org** Internet	<1%
6	**ncbi.nlm.nih.gov** Internet	<1%
7	**University of Sussex on 2011-08-30** Submitted works	<1%
8	**Universiti Tenaga Nasional on 2012-05-18** Submitted works	<1%

turnitin **Similarity Report ID:** oid:27535:17016961

9	University of Lancaster on 2007-01-25 Submitted works	<1%
10	tubdok.tub.tuhh.de Internet	<1%
11	Tayaallen Ramachandran, Mohammad Rashed Iqbal Faruque, Moham... Crossref	<1%
12	Huayu Yang, Yuhao Zhang, Wenhua Gao, Bowen Yan, Jianxin Zhao, Ha... Crossref	<1%
13	University of Bath on 2016-10-25 Submitted works	<1%
14	Mohammad Tariqul Islam, Md. Moniruzzaman, Touhidul Alam, Md Sa... Crossref	<1%
15	bio-protocol.org Internet	<1%
16	N. Amiri, K. Forooraghi, Z. Atlasbaf. "Miniaturized resonant inclusions ... Crossref	<1%
17	Tayaallen Ramachandran, Mohammad Rashed Iqbal Faruque, Moham... Crossref	<1%
18	mafiadoc.com Internet	<1%
19	Higher Education Commission Pakistan on 2010-12-28 Submitted works	<1%
20	Rasheduzzaman Sifat, Mohammad Rashed Iqbal Faruque, Eistiak Ahm... Crossref	<1%

turnitin **Similarity Report ID:** oid:27535:17016961

21	Rutgers University, New Brunswick on 2021-04-30 Submitted works	<1%
22	Sultan Qaboos University on 2016-04-20 Submitted works	<1%
23	Universiti Kebangsaan Malaysia on 2019-05-15 Submitted works	<1%

ACCEPTANCE RECORD

Share your article [MATPR_31861] Inbox ×

is@elsevier.com>

Translate message

ELSEVIER

Share your article!

Dear Ms. Meenakshi,

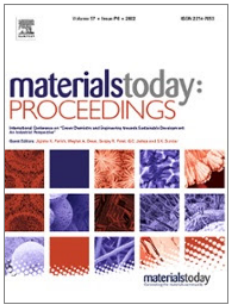

We are pleased to let you know that your article *Design and Simulation of metamaterial under the THz frequency for short-range wireless communication and Military purposes* is now available online with author corrections incorporated. Full citation details, e.g. volume and/or issue number, publication year and page numbers, will be added when the final version becomes available.

To help you access and share this work, we have created a Share Link – a personalized URL providing **50 days' free access** to your article. Anyone clicking on this link before **June 15, 2022** will be taken directly to the latest version of your article on ScienceDirect, which they are welcome to read or download. No sign up, registration or fees are required.

Your personalized Share Link:
https://authors.elsevier.com/a/1ezrM7tbNaNuDU

Click on the icons below to share with your network:

ACKNOWLEDGEMENT

We would like to express our heartfelt gratitude to our mentor, **Dr. Kamal Kishor and Dr. Yogita Kalra** for his keen interest and valuable guidance throughout the course of this project. Their constructive advice and constant motivation have been instrumental in the completion of our venture.

We thank profusely to all the teachers and staff of the *Department of Applied Physics, DTU* for providing us the opportunity to prepare this project.

We also want to express our deep sense of gratitude to Mr. Monu Nath Baitha (Yonsei University, South Korea), Mr. Ankit and Ms. Purnima for valuable guidance throughout the project.

We would also like to thank our classmates for their constant support and valuable inputs at critical junctures during the completion of this project.

.
Meenakshi (2K21/MSCPHY/12)

Prashant (2K21/MSCPHY/21)

TABLE OF CONTENTS

LIST OF FIGURES & TABLE

FIGURES

TABLE

ABSTRACT

This work analyses and designs a new leaf-like metamaterial structure constructed of copper material in the frequency range of 1-10 THz. The suggested metamaterial has a geometrical size of 10 x10 μm^2 and is designed on a FR-4 substrate with a thickness of 0.35 µm. The NRW method is used to calculate the designed structure's permittivity ($\boldsymbol{\varepsilon}_r$), permeability ($\mu_r$), and refractive index (n_r) using scattering parameters. The simulations analysed two different resonance peaks for the transmission (S_{21}) and reflection coefficient (S_{11}) at frequencies of 2.46 THz, 7.83 THz, and 3.15 THz, 8.7 THz, respectively.

In this research, the distribution of electric and magnetic fields is also studied. The proposed structure's effective medium ratio (EMR) is 12.1, that demonstrating the compactness and homogeneity of the proposed metamaterial unit cell. The proposed structure can be used in short-range wireless THz communication or ultrafast THz interconnects, as well as the non-destructive detection of hidden weapons, because it resonates in the THz frequency band.

Here, we have made design on COMSOL Multiphysics software.

CHAPTER - 01

INTRODUCTION

In the exploration of such kind of materials that can manipulate electromagnetic waves, the search began at the end of the 19th century by Jagdish Chandra Basu. After that in the 1940s Winston E. Kock from AT &T laboratories started developing materials by studying their dielectric properties which can manipulate the EM wave. These materials are now known as metamaterials.[1]

Metamaterials are specially engineered materials having some extraordinary properties that are not found in naturally occurring materials. But their base materials do not define their properties until they are designed in some structural form.[2]

Metamaterials can manipulate the em wave by absorbing, blocking, or bending them with their shape, size, geometry and orientation to achieve results that are uncommon in conventional metamaterials.[3]

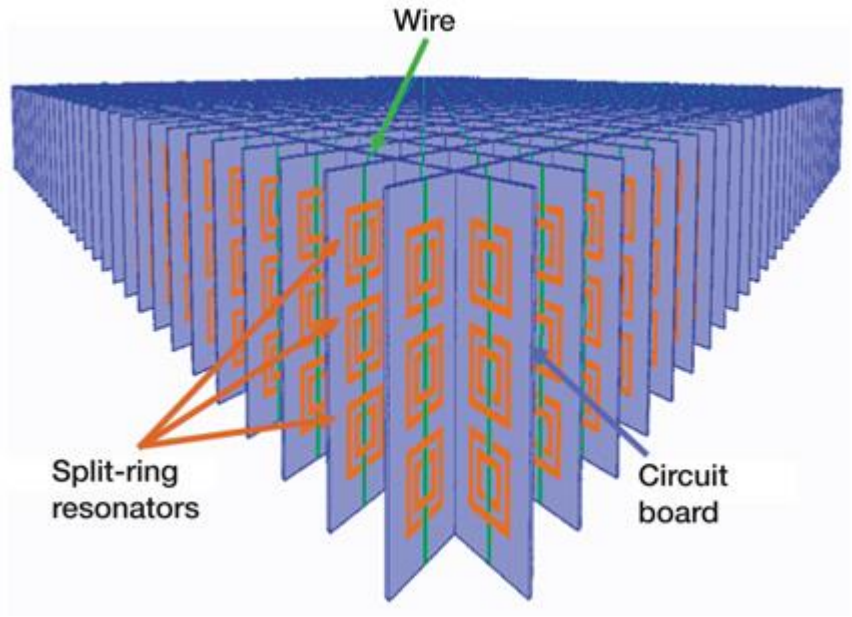

Fig 1: Metamaterial array [1]

Now a days metamaterials are used in various fields like aerospace application, optical filters, high gain antennas, solar power management, etc, and on the basis of these applications' metamaterial possess various properties. Such an extraordinary property is that they show negative refractive index for particular wavelengths and these materials are called negative refractive index metamaterials (NRIs).[4]

The THz frequency ranges from 0.1 to 10 THz has numerous applications in metamaterial research which lies between the microwave and infrared region [5]. In comparison to its surrounding microwave and infrared regimes, the lack of THz materials has hampered the development of THz technology for real-world applications at terahertz frequencies, magnetic responses (permeability) can be measured using a structure made up of non-magnetic elements, such as copper-wire SRR, which show distinct responses centred around a resonant frequency. SRR have demonstrated the ability to tune in the terahertz range. It is the least studied frequency range in the electromagnetic spectrum, despite the fact that it has a wide range of uses, including secure short-range wireless communication, material characterisation, chemical and biological spectroscopy, and sensing. THz metamaterials are discussed here, including their design, fabrication, and characterisation, with a focus on their passive and active features for THz

device applications [6]. A multimode self-resonance enhanced wideband meta surface is presented in year 2021 [7]. This meta surface improves the wireless power system efficiency up to 39.2 % which was 0.04 %. With the meta surface the figure of merit (FoM) is improved to 2.09 at 90 MHz and 2.16 at 770 MHz, respectively.

A metamaterial-based absorber for terahertz based on the dielectric layer of polyimide having a H-shaped slot in the metallic plane which provides absorption peaks at 0.81 THz, 1.98 THz, 3.25 THz and 3.50 THz, respectively [8]. Tunable epsilon negative near zero index metamaterial based on symmetric resonators with high effective medium ratio for multiband wireless applications [9] offers a cross-coupled resonator-based metamaterial for satellite and RADAR communications with negative permittivity, close to zero refractive index, and an EMR of 8.03. On the other hand, a magnetically resonant meta surface with a high Q value which consist of a sandwich structure of Au film, a SiO_2 pacer layer and an Au nanorod array to enhance the Q-value. A metamaterial based on FR-4 substrate material is constructed for long range radio communications showing resonance frequencies at 2.89 GHz, 9.42 GHz and 15.16 GHz [10]. A metamaterial absorber made of tungsten film layered on silicon oxide (SiO_2) is described in another paper [11]. The absorptivity of the MTM is determined by the tungsten nanohole radius [12].A SRR on ultrathin Silicon Nitride (S_iN_x) substrate of thickness 400 nm is designed based on the planar terahertz metamaterial having resonance at 0.255 THz was detected in this SRR-MMs [13].

In this paper, a new design of leaf like metamaterial is designed for the frequency range of 1-10 µm. The scattering parameters (S_{21}) shows the two resonance frequency dips at 2.46 µm and 7.83 µm, respectively. The relative permittivity (ε_r), relative permeability (μ_r) and refractive index (η) is also evaluated. The EMR of the proposed structure comes out to be 12.1.

CHAPTER - 02

APPLICATIONS

2.1 Invisibility cloaking

In invisibility cloaking, Metamaterials alter the path travelled by light via a revolutionary optical material by directing and controlling the propagation and transmission of a specific portion of the light spectrum, displaying the capacity to make an item almost invisible.

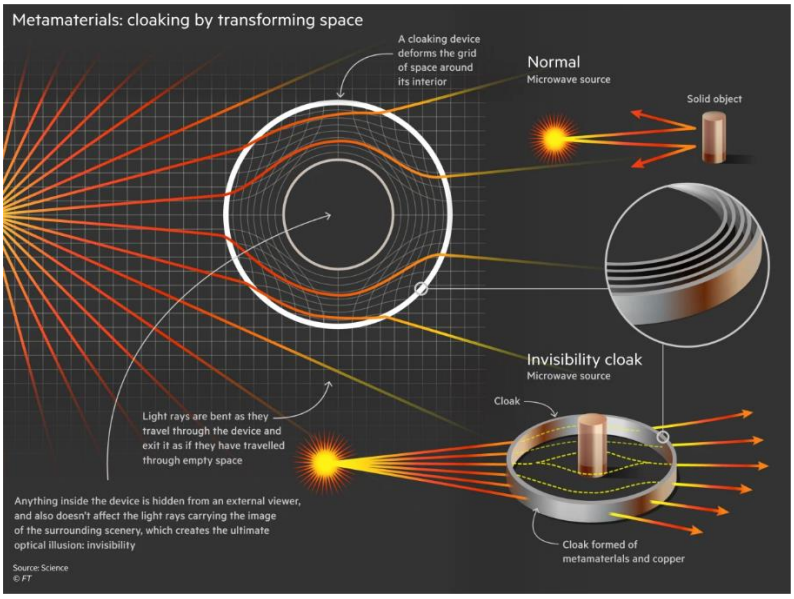

Fig 2: Invisibility cloaking [2]

2.2 Antennas

The majority of the signal is reflected back to the source by conventional antennas that are quite modest in comparison to the wavelength. Metamaterials in antenna designs can increase the antenna's radiated power. Since of its novel structure, a metamaterial antenna appears to be much larger than it is because it stores and re-radiates energy. Metamaterials enable smaller antenna elements to span a larger frequency range, allowing space-constrained applications to make better use of available space.

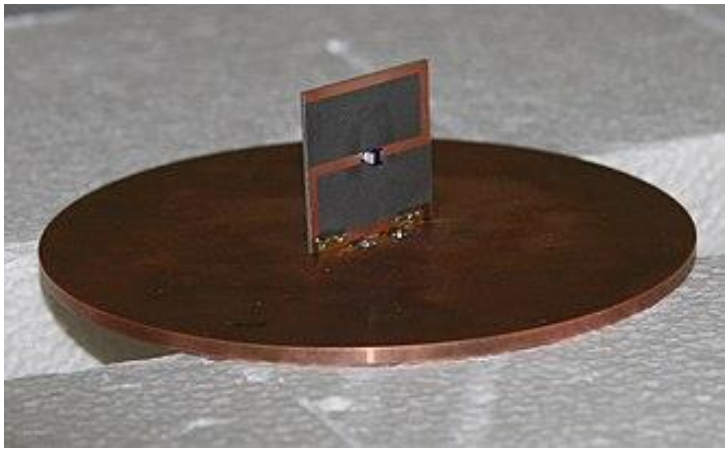

Fig 3: Metamaterial antenna designed by NIST [3]

2.3 Super lenses (Metamaterial lenses)

In the absence of any aberrations, the best optical lens-based imaging systems are purely diffraction-limited. It's long been speculated that physics may be tweaked to increase resolution beyond the limits imposed by the airy disc diameter. Negative refractive index materials were regarded to be a viable option. This is why metamaterials have been proposed for use in the "super lens."

A super lens is a lens that goes above the diffraction limit by using metamaterials. The diffraction limit is a property of traditional lenses and microscopes that restricts their resolution fineness.

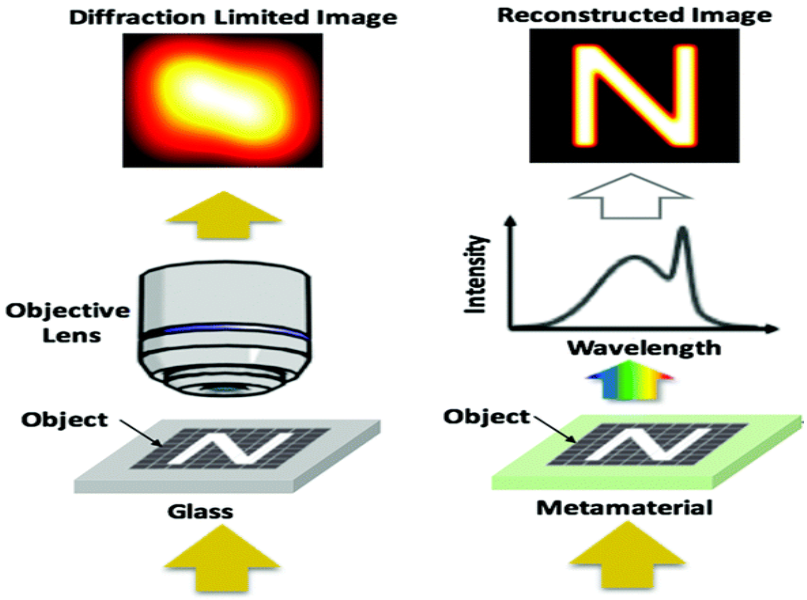

Fig 4: Image reconstruction by metamaterials [4]

2.4 THz Screening for Civil and Military Security

Currently, law enforcement organizations are facing problems in fighting terrorism-related threats. One of the particular interests is the detection of explosives and weaponry hidden beneath the garments The things of particular interest are explosive devices and weapons hidden beneath the clothing. Terahertz electromagnetic waves of frequency from 0.1–3.0 THz are good for this purpose. Explosives like Octogen, Penthrite, and Hexogen exhibit distinct characteristics of transmission and reflection in the THz region that differentiates them from other materials. Radiation from the frequency in THz can also pass-through clothing with little weakening [14] but are highly reflected by metallic objects such as blades, knives, or other weapons [15]. Now as the energy of the photon is very low i.e., 4.4 meV at 1 THz), THz waves offer little health risks to humans and have no effect on the operation of various devices. Strong molecular absorption by water vapour is the principal factor limiting its propagation through the air [15]. Because of the aforementioned characteristics, THz radiation can be mainly used for two security-related applications: bomb detection [16] and person screening [17–19].

CHAPTER - 3

METAMATERIAL PARAMETERS

3.1 Electric and Magnetic field response

An electromagnetic field, which is a physical behaviour formed in space by time-varying electric charges and represents the interaction between electric fields and magnetic fields. Unlike static charges, which can only produce static electric fields in space. The time-varying electric field which is produced by the magnetic fields is one of the cause of time varying electric chThis is described by four differential equation which expressed the time-varying Maxwell's equations.

$$\nabla . E = \rho_v(t)/\varepsilon \qquad \textbf{(3.1 1)}$$

$$\nabla . B = 0 \qquad \textbf{(3.1 2)}$$

$$\nabla \times E = -\mu \frac{\partial H}{\partial t} \qquad \textbf{(3.1 3)}$$

$$\nabla \times B = J(t) + \varepsilon \frac{\partial E}{\partial t} \qquad \textbf{(3.1 4)}$$

Here, ρ_v = charge density of time-varying volume

ε = Relative Electric permittivity

μ = Relative Magnetic permeability

J = Electric current density in a material that varies over time

D & **B** denote the flux densities of the electric and magnetic fields, respectively.

E & **H** denote the intensity of time-varying electric and magnetic fields that varies with time, respectively.

James Maxwell in 1865 developed Equations. from (3.1 1) to (3.1 4) explaining that magnetic fields and oscillating electric fields produces electromagnetic radiation and the speed of these electromagnetic radiations are equivalent to the speed of light in free space. It is equally convenient to demonstrate electromagnetic wave propagation using the curl of Eqs. (3.1 3) and (3.1 4). In addition to conductivity, two primary factors, also known as constitutive parameters, influence the characteristics and behavior of an electromagnetic wave in a material. These are electric permittivity and magnetic permeability. To placed it in another way, the aforementioned characteristics establish the medium's reaction to an incoming electromagnetic wave while paired with the medium's boundary conditions. The following are two equations that represents the electric and magnetic field variable relations in a basic linear and isotropic medium

$$D = \varepsilon E \qquad \textbf{(3.1 5)}$$

$$B = \mu H \qquad \textbf{(3.1 6)}$$

Where each ε and μ are generally complex and frequency-based in a lossy dispersive medium and the real quantities is in the lossless isotropic medium in Eqs. (3.1 5) and (3.1 6). We can calculate some

important parameters like refractive index, n, wavenumber, k by using Eqs. (3.1 1)–(3.1 6), which are given as

$$\boldsymbol{k = \omega\sqrt{\mu\varepsilon}} \qquad \textbf{(3.1 7)}$$

$$\boldsymbol{\eta = \sqrt{\mu\varepsilon}} \qquad \textbf{(3.1 8)}$$

$$\boldsymbol{n = \sqrt{\mu_r\varepsilon_r}} \qquad \textbf{(3.1 9)}$$

Where,

$\boldsymbol{\omega = 2\pi f}$ is the radial frequency (in rad/sec), f is the frequency in Hz

$\boldsymbol{\mu_r = \mu/\mu 0}$ and $\boldsymbol{\varepsilon_r = \varepsilon/\varepsilon 0}$ are the relative permeability and permittivity, respectively.

.

3.2 Negative refractive index (NRIs):

NRIs were first discussed by victor Veselago in 1967 where he showed that it is possible to reverse the direction of phase velocity antiparallel to the pointing vector. We also refer these NRI metamaterials as left-handed metamaterials.

John Pendry in the year of 2000 figure out a practical way to use the left-handed metamaterials, which will allow the EM wave's phase velocity to propagate against the group velocity by aligning a metallic wire along the direction of the wave in a result of which it will provide negative permittivity.

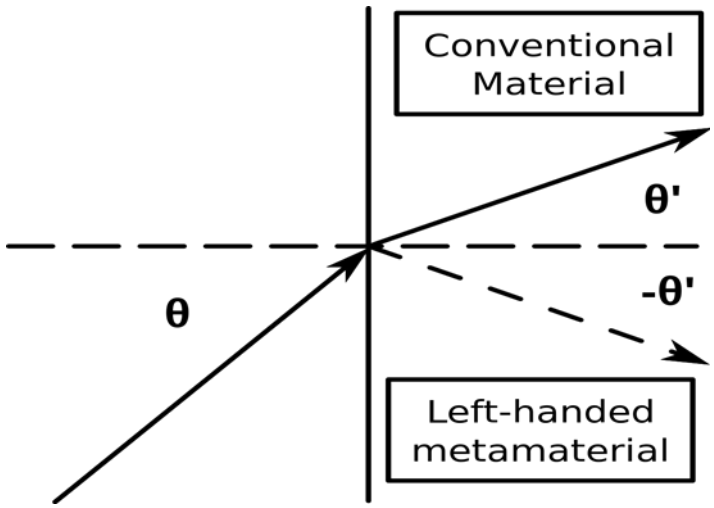

Fig 5: Bending of light through material [5]

From the figure [2] when the light is incident on the interface of the medium then if the material is a conventional material, then the light will get refracted in positive θ direction in the reference of the normal and if the material is a NRI material then the light will get reflected in $-\theta$ direction.

In optics, a material's refractive index is generally considered as a measure of its 'optical density,' and is defined as

$$\mathbf{n = c\ v} \qquad \textbf{(3.2 1)}$$

Where,

c stands for the vacuum speed of light.

In a medium, v is the velocity of an electromagnetic plane wave.

The Maxwell relation, derived from Maxwell's equations, determines the refractive index

$$\boldsymbol{n^2 = \varepsilon\mu} \qquad \textbf{(3.2 2)}$$

ε = the relative dielectric permittivity

And μ = the relative magnetic permeability of the medium.

$$\boldsymbol{n = \sqrt{\mu_r \epsilon_r}} \qquad \textbf{(3.2 3)}$$

Now, negative refraction can be achieved when ($\boldsymbol{\mu_r}$ *and* $\boldsymbol{\epsilon_r}$) are negative.

$$\begin{aligned}\sqrt{(-\boldsymbol{\mu_r})(-\boldsymbol{\epsilon_r})} &= \sqrt{\boldsymbol{e^{-j\pi}}} \times \sqrt{\boldsymbol{e^{-j\pi}}} \times (\sqrt{\boldsymbol{\mu_r \epsilon_r}}) \\ &= (\boldsymbol{e^{-j\pi/2}}) \times (\boldsymbol{e^{-j\pi/2}}) \times (\sqrt{\boldsymbol{\mu_r \epsilon_r}}) \\ &= \boldsymbol{e^{-j\pi}} \times (\sqrt{\boldsymbol{\mu_r \epsilon_r}}) \\ &= \boldsymbol{-1} \times (\sqrt{\boldsymbol{\mu_r \epsilon_r}})\end{aligned}$$

The sole issue was to obtain negative permeability, as all natural materials have negative permittivity.

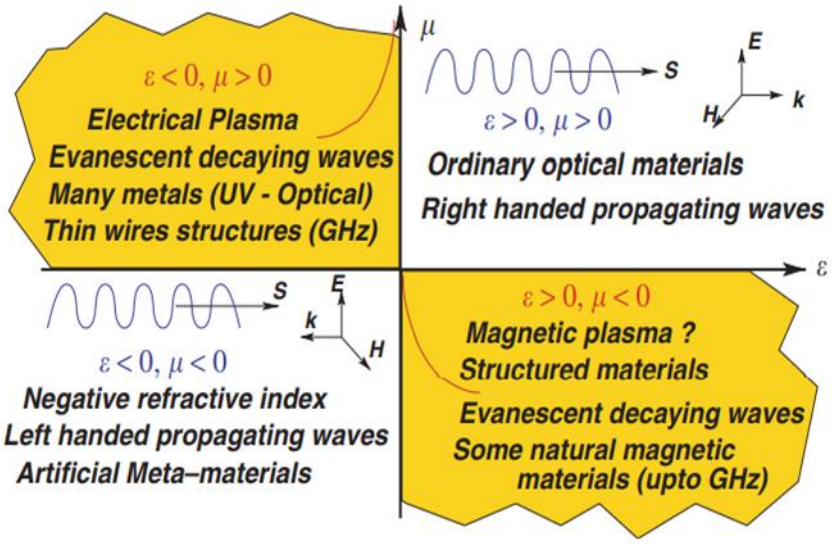

Fig6: Categories of materials according to their ϵ and μ [6].

3.3 Phase velocity, group velocity and energy flow:

In an isotropic NRM negative refraction is achieved by the wave vector that that points in the opposite direction of the Poynting vector $\boldsymbol{S} = \boldsymbol{E} \times \boldsymbol{H}$.The phase velocity $\boldsymbol{v_\varphi} = \boldsymbol{k}/\boldsymbol{\omega}$ is plainly negative as a result. However, the energy flow is away from the source and along the Poynting vector.

The group velocity, given as $\boldsymbol{v_g} = \boldsymbol{\nabla_k \omega(k)}$, for relatively narrow-band pulses, is generally along the direction of the Poynting vector and should thus be oriented opposite to the phase velocity. However, for broad-band pulses that are easily twisted due to dispersion, the concept of a group velocity may fail. In anisotropic media, the pointing vector and the phase velocity can both point in opposite directions. As a result, we shouldn't be surprised by this point.

In an NRM the group velocity and negative refraction effect have been the topic of some heated discussion. It was supposed that refraction at the interface between a positive medium and an NRM was positive. In a homogeneous isotropic medium, the group velocity is

$$\boldsymbol{v_g = \nabla_k \omega(k) = p\hat{k}\,\frac{d\omega(k)}{dk}}$$

Both the phase velocity and the Poynting vector can be used in anisotropic media.

Here $\boldsymbol{p = \pm 1}$, due to isotropy. This indicates that the group velocity can only be anti- parallel to or parallel to the phase velocity (in a positive medium) (in an NRM).

3.4 S- Parameters:

At various ports of devices such as filters, antennas, waveguide transitions, and transmission lines scattering parameters (S-parameters) are matrices which are used to describe the transmission and reflection of electromagnetic waves

For a device having n ports, the S-parametersis given by,

$$\boldsymbol{S} = \begin{bmatrix} \boldsymbol{S_{11}} & \boldsymbol{S_{12}} \cdots & \boldsymbol{S_{1n}} \\ \vdots & \ddots & \vdots \\ \boldsymbol{S_{n1}} & \cdots & \boldsymbol{S_{nn}} \end{bmatrix}$$

Where, $\boldsymbol{S_{21}}$ gives the transmission coefficient from port 1 to port 2, and $\boldsymbol{S_{11}}$ gives the reflection coefficient at port 1 . The time average power reflection/transmission coefficients are obtained as$|\boldsymbol{S_{ij}}|^{\boldsymbol{2}}$**.**

The scattering parameters can be used to analyse the MTM influence on wave propagation. The S-parameters correspond to reflection coefficients when impedance matching is taken into account. As a result, analysing those parameters provides crucial information on the guide's propagation quality. The lowest possible reflection coefficient signifies the best possible signal transmission within the stated objectives. High transmission rates are represented by low reflection indices.

The transmission coefficient (S_{21}) and reflection coefficient (S_{11}) are used to calculate metamaterial properties like relative permeability and relative permittivity.

The simplified formulas for the calculation are given below [11]:

$$\boldsymbol{\varepsilon_r} = \frac{\boldsymbol{2}}{\boldsymbol{jkd}} \frac{\boldsymbol{1-S_{11}-S_{21}}}{\boldsymbol{1+S_{11}+S_{21}}} \qquad \textbf{(3.4 1)}$$

$$\boldsymbol{\mu_r} = \frac{\boldsymbol{2}}{\boldsymbol{jkd}} \frac{\boldsymbol{1+S_{11}-S_{21}}}{\boldsymbol{1-S_{11}+S_{21}}} \qquad \textbf{(3.4 2)}$$

$$\boldsymbol{n} = \frac{\boldsymbol{2}}{\boldsymbol{jkd}} \sqrt{\frac{\boldsymbol{(S_{21}-1)^2-(S_{11})^2}}{\boldsymbol{(S_{21}+1)^2-(S_{11})^2}}} \qquad \textbf{(3.4 3)}$$

Where, η = Refractive index
C = Velocity of light
d = Slab Thickness

CHAPTER - 4

DESIGN OF METAMATERIAL

Metamaterial design plays an important role in achieving the desired properties. To design a metamaterial, we take the dimension of metamaterial to be much smaller than the wavelength. This property makes metamaterial structure a special structure. Proposed metamaterial will be finalized through step by step design and observing the response of different properties to different design configurations.

4.1 Metamaterial structure

As shown in Fig. 1, the suggested metamaterial's unit cell is made of FR-4 dielectric substrate material with a dimension of 10 x 10 μm^2 and a thickness (t_1) of 0.8 µm, with tangent loss (δ) of 0.02 and dielectric constant (ε) of 4.4. The proposed structure was composed of copper material with a conductivity (σ) of 5.80 107 S/m, and the thickness was determined to be 0.35 µm from the substrate's surface. A square ring with outer and inner side dimensions of 10 µm and 9 µm was first constructed on the substrate, and within this square ring, a gap of 0.5 µm 0.16 µm was created, and two rectangles and eight triangles were arranged to construct a leaf-like design. The standard copper material structure, which was structured like a leaf, had a thickness of 0.35 µm. The Outer rectangle has dimensions as 7 × 0.3 µm whereas the inner rectangle has 2.2 µm × 0.4 µm. Then we have eight triangles, with the lower triangles having the same dimensions as the upper triangles. Upper triangle as shown in Fig. 1(a) and dimension of these triangles shown in Table 1.

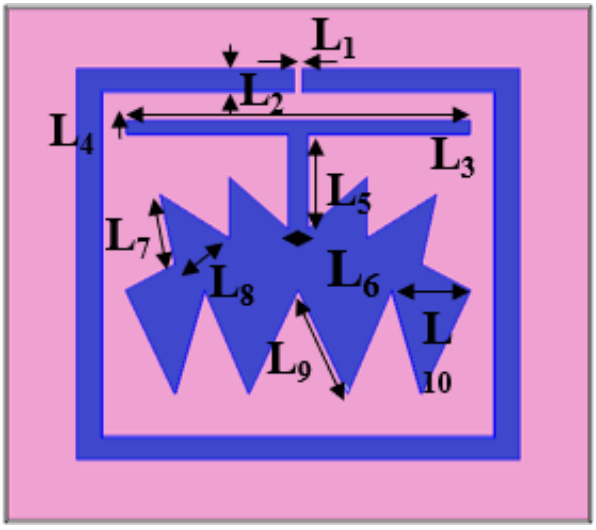

Fig 7: Front view of Proposed Metamaterial

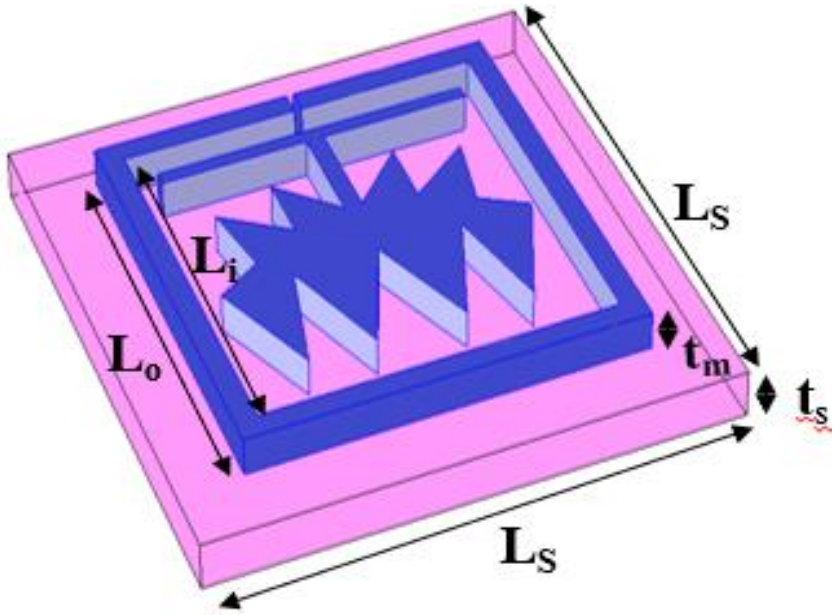

Fig 8: Side View of Metamaterial

Parameters	Dimension (μm)	Description
L_0	9.0	Outer square ring side
L_i	8.0	Inner square ring side
L_1	0.5	Gap width
L_2	1.6	Gap height
L_3	7.0	Outer rectangle length
L_4	0.3	Outer rectangle breadth
L_5	2.2	Inner rectangle breadth
L_6	0.4	Inner rectangle length
L_7	1.6	Upper triangle side
L_8	1.2	Upper triangle base
L_9	2.6	Lower triangle side
L_{10}	1.6	Lower triangle base
L_s	10	Length of substrate
t_1	0.8	Substrate thickness
t_2	0.35	Material thickness

Table 1: Parameters with dimension of designed unit cell

4.2 Constitution of metamaterial

We used a FR-4 substrate in the proposed metamaterial. With a loss tangent of 0.02 and a permittivity of 4.4, FR-4 has the highest permittivity. On the other hand, Rogers has the lowest permittivity of 2 and a loss tangent of 0.0021. FR-4 is also cost friendly that why this is good for our proposed metamaterial.

The choice of substrate material plays a vital role in metamaterial unit cell design because for the electromagnetic field, the resonant excitation which is determined by the exact geometrical shape of the conductive materials deposited on the dielectric substrate material, is crucial to the functionality of those metamaterials. The resonance frequency and electromagnetic characteristics of metamaterial unit cells are affected by the substrate. In macroscopic terms, resonant excitation changes effective optical characteristics like the dielectric constant and magnetic permeabilities.

The refractive index of the substrate which acts like a support for the metamaterial and which changes the effective size of the metamaterial patterns, affects the resonant frequency of metamaterial.

Dielectric constant: It describes the ratio of the permittivity of the substance to the permittivity of the free space.

$$\boldsymbol{K} = \frac{\boldsymbol{\varepsilon}}{\boldsymbol{\varepsilon o}}$$

Were,

$\boldsymbol{\varepsilon}$ and $\boldsymbol{\varepsilon o}$ are permittivity of material and free space respectively**.**

Permittivity: It is the measure of a material that is concerned with the polarization of that material

Permeability: It is the measure of a material which is concerned with the magnetization of that material.

Loss tangent: It is the measure of the dissipation of electromagnetic energy in the substrate of the metamaterial. It is also referred as dissipation factor. It is given by

$$\mathbf{D} = \mathbf{tan}\,\boldsymbol{\delta},$$

Where δ is the loss angle

$$\mathbf{tan}\,\boldsymbol{\delta} = \frac{\boldsymbol{\varepsilon}^{\mathbf{I}}}{\boldsymbol{\varepsilon}^{\mathbf{R}}}$$

Where $\boldsymbol{\varepsilon^I}$ **and** $\boldsymbol{\varepsilon^R}$ **are** imaginary and real parts of the dielectric constant respectively.

CHAPTER - 5

RESULTS AND DISCUSSION

5.1 Estimation of S-Parameter and electromagnetic parameters

The evaluation of scattering parameter is done in RF module Finite element method based on COMSOL Multiphysics simulation software. The direction of propagation of the electromagnetic plane wave is along the z-axis and the Perfect Magnetic Conductor and Perfect Electric Conductor boundary condition is applied along the y-and x-axis with electric field polarized along y- axis. The Nicolson–Ross–Weir approach is used for the calculation of effective medium parameters i.e., permittivity (ε), permeability (μ) and refractive index (η) of the proposed structure.

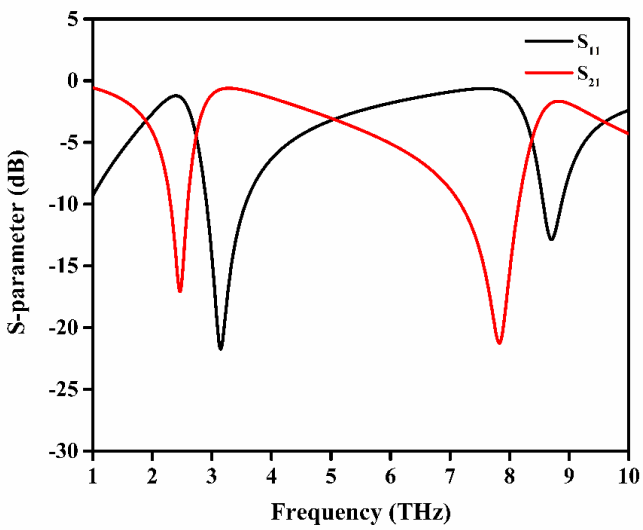

Fig 9. Scattering parameter (S_{11} & S_{21}) variation with the incident frequency wave.

The transmission coefficient ($\boldsymbol{S_{21}}$) and reflection coefficient ($\boldsymbol{S_{11}}$) of the proposed metamaterial unit cell are illustrated in Fig 2.

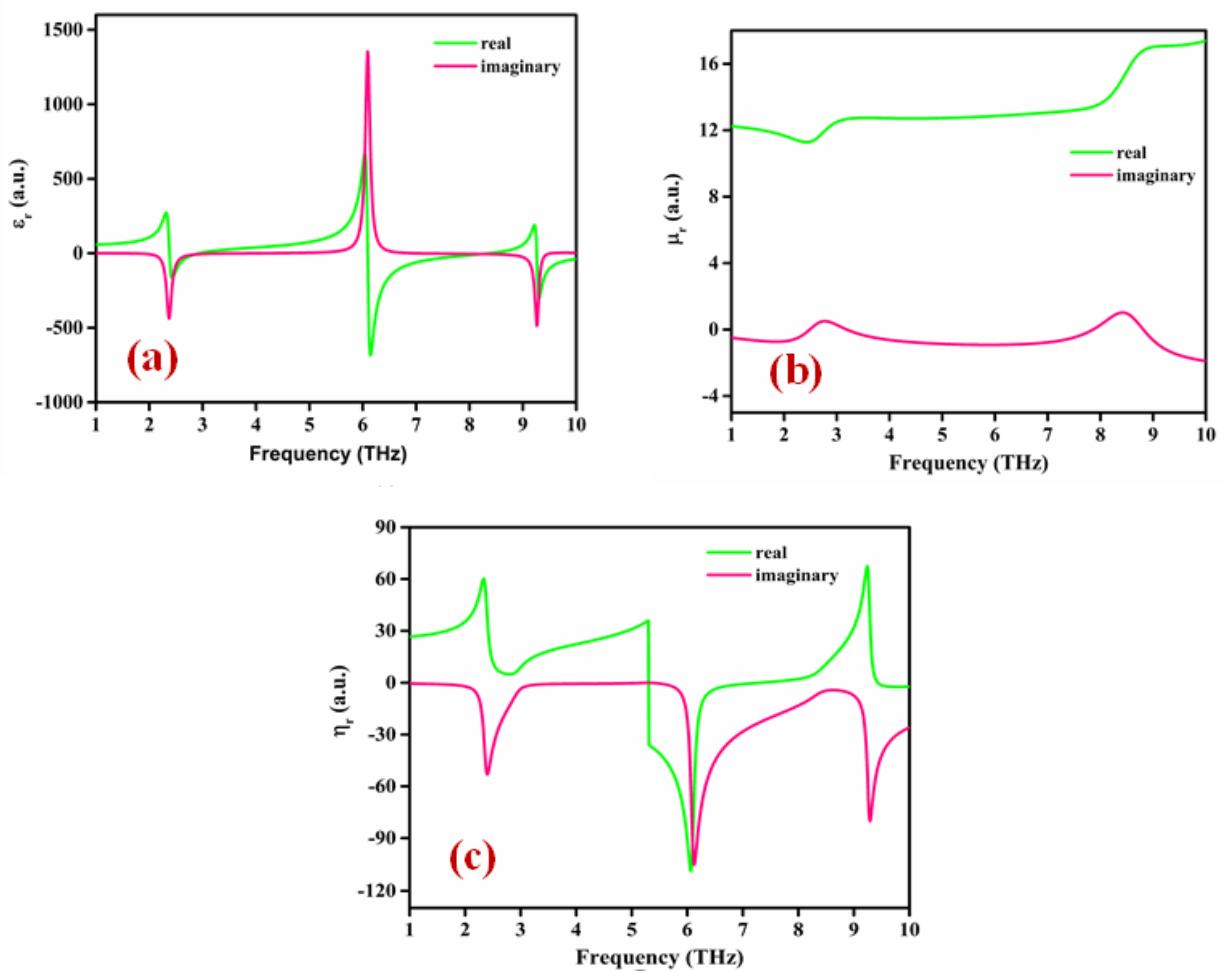

Fig 10: Variation of (a) Relative permittivity (ε_r), (b) Relative permeability (μ_r) and (c) Relative refractive index (η) with the incident wave frequency on the proposed metamaterial unit cell

The transmission coefficient (S_{21}) shows a dip at resonance frequencies 2.46 THz and 7.83 THz with the amplitudes of -17.084 dB and -21.25 dB, correspondingly, similarly the unit cell's reflection coefficient (S_{11}) showed two resonances with amplitudes of -21.74 dB and -12.865 dB at frequencies of 3.15 THz and 7.5 THz respectively. The plot of permittivity (ε), permeability (μ) and refractive index (η) of the proposed metamaterial is displayed in Fig. 3. In Fig. 3(a), the peak corresponding to frequencies 2.4 THz, 6.14 THz and 9.3 THz shows negative permittivity with amplitude -165, -684 and -300 respectively and for permeability there is slight drop on frequency for 2.4 THz as shown in Fig. 3(b) with amplitude 11.27. The negative refractive index is shown on frequencies 6 THz and 9.5 THz with amplitude -108.28 and -2 and positive refractive index on 2.79 THz with amplitude 4.8 (Fig. 3(c)).

5.2 Electric field and Magnetic field distribution

In fig. 12 and 13, Distribution of electric field and magnetic field is shown

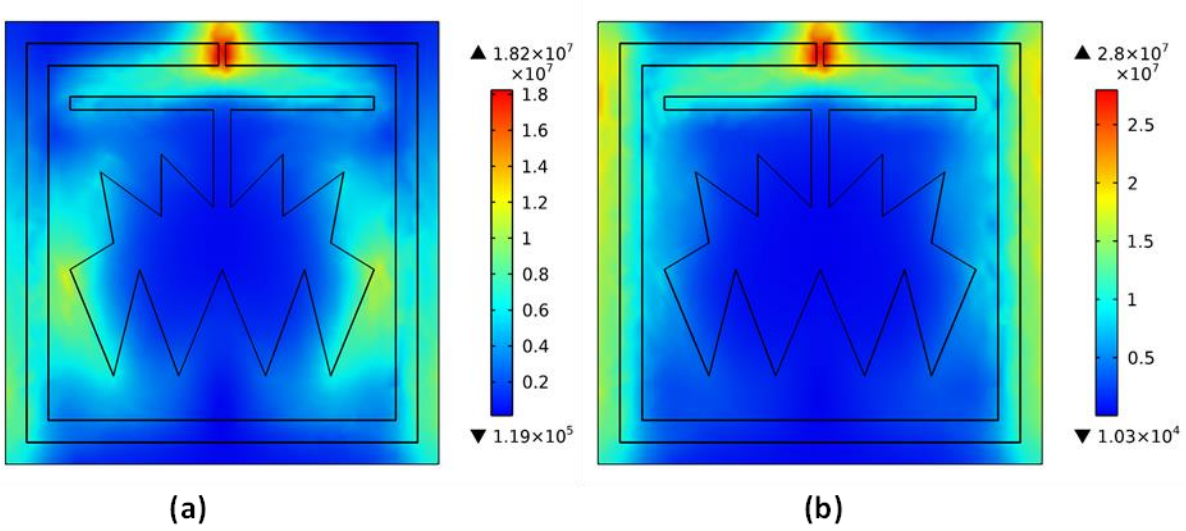

Fig 11. Electric Field at (a) 2.4 THz (b) 7.8 THz

It is seen from the fig. 4 (a) that the electric field concentrates maximum in the gap (L_1) between the square ring of the order of nearly 1.82×10^7 V/m for the frequency 2.4 THz

As the frequency increases to 7.8 THz, the confinement of the electric field in the gap increases to the order of 2.8×10^7 V/m (Fig. 4(b)). With change in frequency there is a change in the electric field distribution caused by the large amount of accumulation of charges causing the metamaterial structure to resonate in the frequency range. The plot of magnetic field distribution for the resonance frequency is presented in Fig. 7.

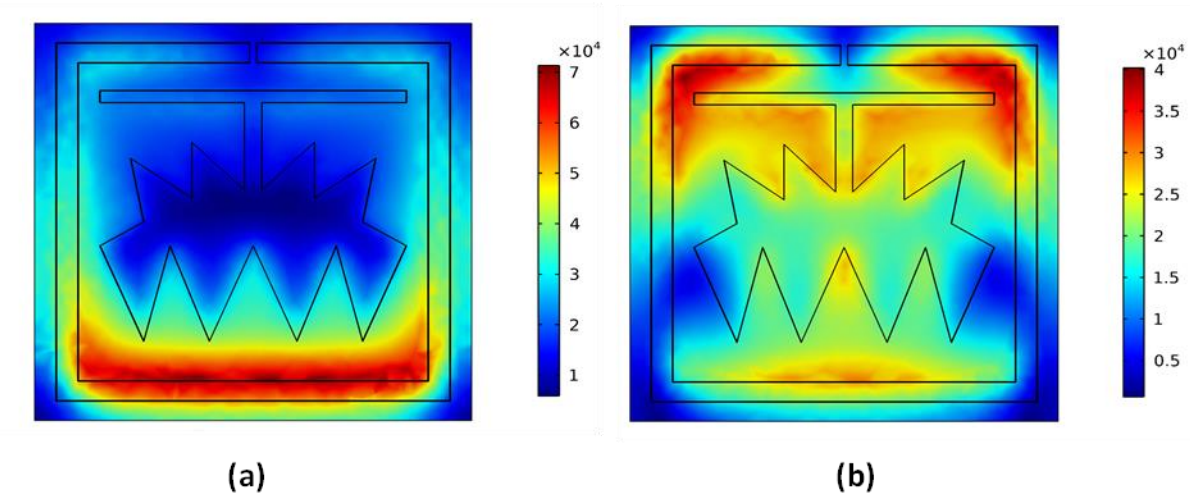

Fig 12: Magnetic Field at (a) 2.4 THz (b) 7.8 THz

The magnetic field accumulate in the lower part of the structure for the resonance frequency 2.4 THz of the order of 7×10^4 A/m but for 7.8 THz the accumulation is in both upper and lower part of the structure.

5.3 FAR FIELD RADIATION PATTERN

Far Field Region, also known as Radiation Field, it is the area that follows the near radiative near field. Radiating fields are used to control the electromagnetic fields in this area. As the plane waves, the E and H-fields are orthogonal to each other and also to the direction of propagation. The below equation represents the far-field area:

$$Far\ Field\ region > \frac{2D^2}{\lambda}$$

Energy of the radiated antenna is represented by the pattern of radiation of an antenna. Pattern of radiation is representations of radiated energy which is distribution in space as the direction function.

(a) Pattern of Radiation

In various direction, the relative strength of the radiated field from the antenna at a constant distance is described by pattern of radiation or antenna. The pattern of radiation is also a "reception pattern," as it describes the antenna's receiving characteristics. The pattern of radiation is three-dimensional, yet displaying the three-dimensional radiation pattern in a meaningful way is problematic manner. Measuring a three-dimensional radiation pattern takes time as well. Often, the patterns of radiation detected are 2-D representation of the 3-D pattern, which can be conveniently presented on a screen or sheet of paper. These Pattern measurements can be displayed in a rectangular or polar style.

(b) Directivity

It is an antenna's ability to focus energy in a certain direction when transmitting or to receive energy more efficiently from a specific direction when receiving. The ratio of the antenna's peak radiation intensity to the isotropic or reference antenna radiating the same total power is known as directivity.

Antennas radiate power, but the direction in which they transmit it is crucial. The antenna whose performance is being evaluated is known as the subject antenna. While sending or receiving, the intensity of its radiation is directed in a specific direction.

(c) Lobe Formation

We frequently come across distinct shapes in the representation of a radiation pattern, which show the major and minor radiation zones, which are used to determine the antenna's radiation effectiveness.

Now following is the diagram of the dipole antenna radiation pattern

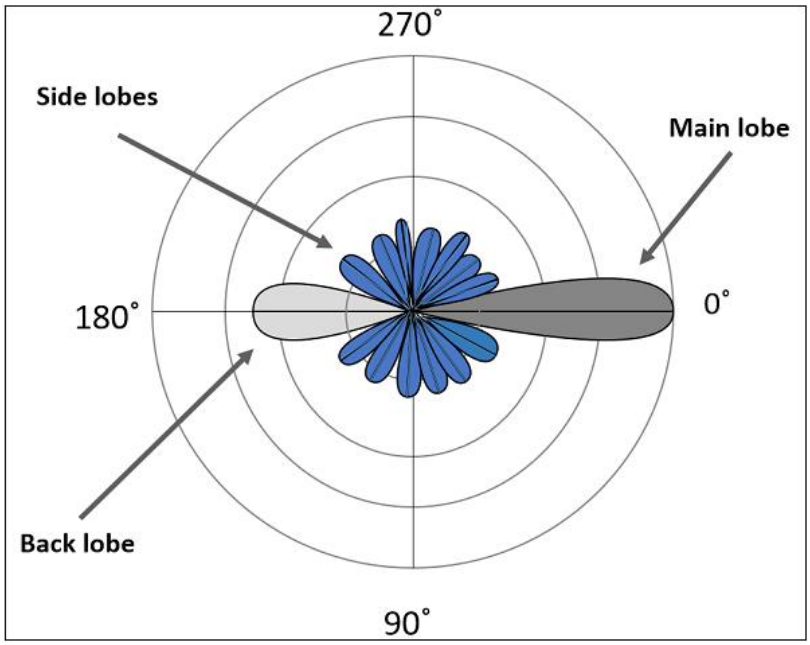

Fig 13: Lobe

There is a main lobe, side lobes, and back lobe in this radiation pattern.

- The major lobe is the main lobe which has the most extensive part of the radiated field, which spans in a larger area and which has the most extensive part of the radiated field and this is the portion where all the energy is released. Because of the orientation of this lobe the antenna's directivity is determined
  .
- The other lobe is in the opposite direction of the first lobe which is known as black lobe or minoe lobe.. A large amount of energy is lost even here.

The Far field radiation pattern for the resonance frequencies 2.4 THz and 7.8 THz is shown in Fig. 6. The far field radiation pattern shows that the lobe is distributed on the vertical axis at 2.46 THz frequency, demonstrating unidirectionality, but as the frequency increases to 7.8 THz, the lobe reduces to a single lobe. The proposed structure's directivity is 2.856 dB, indicating that the designed structure can be implemented as an antenna with the appropriate directivity.

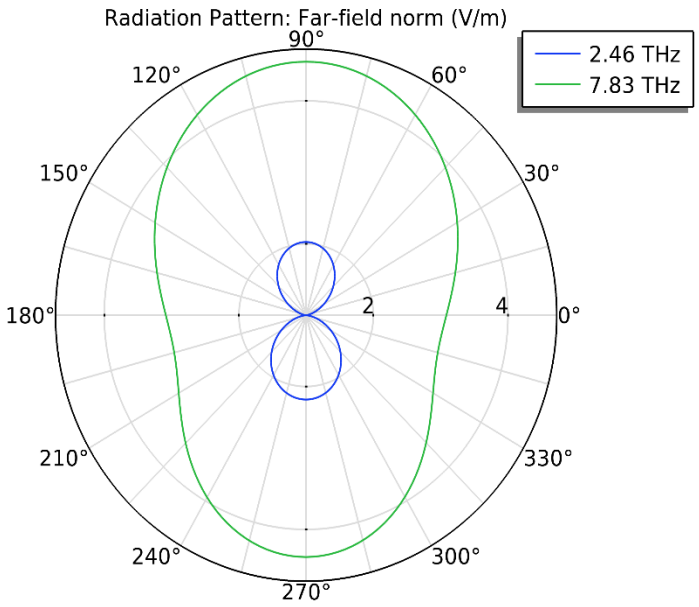

Fig.14: Far Field radiation pattern of the designed structure

5.4 Effective Medium Ratio (EMR)

The metamaterial size structure is miniaturised and follows a suitable EMR.The effective medium ratio (EMR) is a crucial factor for a metamaterial's properties, since it symbolises the metamaterial's compact size and efficiency [11]. Many devices work at low resonance frequencies, but due to the small size of metamaterial, low resonance frequencies are difficult to achieve, but a high EMR symbolises the metamaterial design's perfection and criteria fulfilment. If the EMR value is more than 4, negative permittivity is possible with the proposed metamaterial design. If the EMR value is less than 4, the metamaterial sub wavelength condition is not met. Following is the simplified formula for calculating the EMR:

$$EMR = \frac{Operating\ wavelength\ of\ unit\ cell\ (\lambda)}{Unit\ cell\ length\ (L)}$$

The computed EMR value for the proposed metamaterial unit cell is 12.1 (10×10×1.15). The high EMR value demonstrates the structure's compactness.

CHAPTER - 6

CONCLUSION

For THz applications in the range of 1-10 THz, a new leaf-like metamaterial structure is designed and investigated. In addition, the scattering and propagation parameters are analyzed. For transmission coefficient, the structure resonates at two resonance frequencies i.e., 2.46 THz and 7.83 THz (S_{21}). At 2.46 THz, the structure exhibits negative permittivity. Also exhibited is the electric and magnetic field response at the resonance frequency. Because the suggested metamaterial unit cell is tiny, it achieves the ideal resonance frequency and a high EMR value of 12.1. The antenna structure can be used with a computed directivity value. As a result, the proposed metamaterial can be used in short-range wireless THz communication, ultrafast THz interconnects, and non-destructive detection of hidden objects.

FIGURE CITATION

[1]https://upload.wikimedia.org/wikipedia/commons/f/fb/Lefthanded_metamaterial_array_configuration.jpg

[2] Science report , Hong Kong University of Science and Technology, “Invisibility cloak’ metamaterials make their way into products "by Josh Jacobs MARCH 29 2018.

[3] https://pubs.rsc.org/en/content/articlelanding/2017/nr/c7nr05436j/unauth

[4]https://en.wikipedia.org/wiki/Metamaterial_antenna#/media/File:Z_Antennas_at_UHF Frequencies.jpg

[5] https://en.wikipedia.org/wiki/Negative_refraction#/media/File:Metarefraction.svg

[6] S. P. Burgos, R. De Waele, A. Polman, and H. A. Atwater. A single- layer wide-angle negative-index metamaterial at visible frequencies. Nature Materials, 9(5):407–412, 2010F. Capolino. Theory and phenomena of metamaterials. CRC press, 2017.

[7,8,9,10,11,12] Comsol Multiphysics software .

[13]https://www.tutorialspoint.com/antenna_theory/antenna_theory_near_and_far_fields.htm

[14] Comsol Multiphysics software

SCOPUS INDEXED REPORT

ScienceDirect Journals & Books Register Sign in

View PDF

Outline

Abstract
Keywords
1. Introduction
2. Design of the unit cell structure
3. Result and discussion
4. Conclusion
Declaration of Competing Interest
Acknowledgments
References

Show full outline

Cited By (0)

Figures (6)

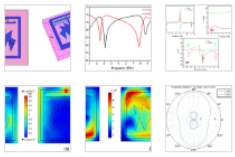

materialstoday: PROCEEDINGS
Available online 26 April 2022
In Press, Corrected Proof

Design and simulation of metamaterial under the THz frequency for short-range wireless communication and military purposes

Meenakshi, Prashant Saurav, Kamal Kishor

Show more

+ Add to Mendeley Share Cite

https://doi.org/10.1016/j.matpr.2022.04.437 Get rights and content

Abstract

A new leaf-like metamaterial structure made up of copper material is analyzed and designed in this paper in the frequency range of 1–10 THz. The suggested metamaterial designed on an FR-4 substrate with a thickness of 0.35 μm having a geometrical dimension of $10 \times 10\ \mu m^2$. The NRW method is used for the calculation of permittivity (ε_r), permeability (μ_r) and refractive index (η_r) of the designed structure with the help of scattering parameters. Two resonance peaks for the transmission (S_{21}) and reflection coefficient (S_{11}) discovered in the simulations at

Recommended articles

Ultralow bending-loss micro-structured fiber wi...
Optik, Volume 251, 2022, Article 168440
Download PDF View details

Laser-irradiated graphene-polymer contact elec...
Materials Today: Proceedings, Volume 57, Part 1, 2022,...
Download PDF View details

Micro-structural and temperature dependent el...
Current Applied Physics, Volume 13, Issue 6, 2013, pp. ...
Purchase PDF View details

1 2 Next

Article Metrics

Social Media

Tweets: 1

PLUMX View details

Activate Wind
Go to Settings to a

REFERENCES

[1] D. R. Smith, J. B. Pendry, and M. C. Wiltshire, “Metamaterials and negative refractive index,” Science, vol. 305, no. 5685, pp. 788–792, 2004.

[2] M. Moniruzzaman, M. T. Islam, I. Hossain, M. S. Soliman, M. Samsuzzaman, and S. H. Almalki, “Symmetric resonator based tunable epsilon negative near zero index metamaterial with high effective medium ratio for multiband wireless applications,” Scientific Reports, vol. 11, no. 1, pp. 1–21, 2021.

[3] S. Mingle, I. Hassoun, and W. Kamali, “A combination of c and u double negative metamaterial having negative permittivity and permeability at 28ghz,” in 2018 1st International Conference on Advanced Research in Engineering Sciences (ARES), pp. 1–4, IEEE, 2018.

[4] M. B. Hossain, M. R. I. Faruque, S. S. Islam, and M. T. Islam, “Modified double dumbbell-shaped split-ring resonator-based negative permittivity metamaterial for satellite communications with high effective medium ratio,” Scientific Reports, vol. 11, no. 1, pp. 1–18, 2021.

[5] M. Beruete and I. Jáuregui-López, “Terahertz sensing based on metasurfaces," Adv. Opt. Mater., vol. 8, no. 3, Feb. 2020, Art. no. 1900721

[6] M. J. Fitch and R. Osiander. Terahertz waves for communications and sensing. Johns Hopkins APL technical digest, 25(4):348–355, 2004.

[7] X. Jiang, R. K. Pokharel, A. Barakat, and K. Yoshitomi. A multimode metamaterial for a compact and robust dualband wireless power transfer system. Scientific reports, 11(1):1–10, 2021.

[8] S. C. Bakshi, D. Mitra, and L. Minz. A compact design of multiband terahertz metamaterial absorber with frequency and polarization tunability. Plasmonics, 13(6):1843–1852, 2018.

[9] M. Moniruzzaman, M. T. Islam, I. Hossain, M. S. Soliman, M. Samsuzzaman, and S. H. Almalki. Symmetric resonator based tunable epsilon negative near zero index metamaterial with high effective medium ratio for multiband wireless applications. Scientific Reports, 11(1):1–21, 2021.

[10] W.-Y. Tsai, C.-M. Wang, C.-F. Chen, P. C. Wu, Y.-H. Chen, T.-Y. Chen, P. R. Wu, J.-W. Chen, and D. P. Tsai. Material-assisted metamaterial: a new dimension to create functional metamaterial. Scientific reports, 7(1):1–6, 2017.

[11] H. Tao, A. C. Strikwerda, M. Liu, J. P. Mondia, E. Ekmekci, K. Fan, D. L. Kaplan, W. J. Padilla, X. Zhang, R. D. Averitt, et al. Performance enhancement of terahertz metamaterials on ultrathin substrates for sensing applications. Applied Physics Letters, 97(26):261909, 2010.

[12] M. Moniruzzaman, M. T. Islam, N. Misran, M. Samsuzzaman, T. Alam, and M. E. Chowdhury. Inductively tuned modified split ring resonator based quad band epsilon negative (ε) with near zero index (n) metamaterial for multiband antenna performance enhancement. Scientific reports, 11(1):1–29, 2021.

[13] S. U. Afsar, M. R. I. Faruque, M. J. Hossain, M. U. Khandaker, H. Osman, and S. Alamri. Modified hexagonal split ring resonator based on an epsilon-negative metamaterial for triple-band satellite communication. Micromachines, 12(8):878, 2021.

[14] Gatesman AJ et al (2006) Terahertz behaviour of optical components and common materials. Proc SPIE 6212:62120E

[15] Yun-Shik L (2008) Principles of terahertz science and technology. Springer, New York

[16] Palka N et al (2012) THz spectroscopy and imaging in security applications. 19th international conference on microwaves, radar and wireless communications, pp 265–270

[17] Heinz E et al (2012) Development of passive submillimeter-wave video imaging systems for security applications. Proc SPIE 8544:854402

[18] Cooper KB, Dengler RJ, Llombart N, Bryllert T, Chattopadhyay G, Mehdi I, Siegel PH (2009) An approach for sub-second imaging of concealed objects using terahertz (THz) radar. J Infrared Millim Terahz Waves 30:1297–1307

[19] Appleby R, Wallace HB (2007) Standoff detection of weapons and contraband in the 100 GHz to 1 THz region. IEEE Trans Antennas Propag 55:2944–2956

[20] Millivision, website: www.millivision.com

[21] ProVision ATD, website: http://www.sds.l-3com.com

[22] ThruVision System Ltd., website: www.truvision.com

[23] Brijot imaging systems Inc., website: www.brijot.com

[24] STANAG 4349 (ED. 1) Nato standardization agreement: measurement of the minimum resolvable temperature difference of thermal cameras (09-AUG-1995)

REGISTRATION RECORD

REGISTRATIONFORM

PAPERID: 468

Full Name: Meenakshi

Designation: Student

Organization & Address: Delhi Technological University, Bawana Rd Shahbad Daulatpur Village, Rohini, New Delhi, Delhi 110042

Mobile: 8950672757

E-mail:mmegha848@gmail.com

Amount paid: Materials Today: Proceedings: 9000

Name of the Bank: State Bank of India

Name of the account holder: Sachin

Date of the transaction: 09April, 2022

Online Transaction number: IMPS00199124465

Registration Category: Educational Institution

Signature withDate

Meenakshi
09April, 2022

CorrespondenceAddress:
ICMPC-2022
GOKARAJURANGARAJUINSTITUTE OFENGINEERING&TECHNOLOGY
BACHUPALLY, HYDERABAD-500090 TELANGANA,
INDIA.PHONE.NO:091-9959870257
E-mail:icmpc-hyd@griet.ac.in

Contents lists available at ScienceDirect

Materials Today: Proceedings

journal homepage: www.elsevier.com/locate/matpr

Design and simulation of metamaterial under the THz frequency for short-range wireless communication and military purposes

Meenakshi *, Prashant Saurav, Kamal Kishor

TIFAC- Centre of Relevance and Excellence in Fiber Optics and Optical Communication, Department of Applied Physics, Delhi Technological University, Bawana Road, Delhi 110042, India

ARTICLE INFO

Article history:
Available online xxxx

Keywords:
Effective Medium Ratio (EMR)
Metamaterial (MTM)
Permittivity
Permeability
Refractive index

ABSTRACT

A new leaf-like metamaterial structure made up of copper material is analyzed and designed in this paper in the frequency range of 1–10 THz. The suggested metamaterial designed on an FR-4 substrate with a thickness of 0.35 μm having a geometrical dimension of 10 × 10 μm^2. The NRW method is used for the calculation of permittivity (ε_r), permeability (μ_r) and refractive index (η_r) of the designed structure with the help of scattering parameters. Two resonance peaks for the transmission (S_{21}) and reflection coefficient (S_{11}) discovered in the simulations at frequencies of 2.46 THz, 7.83 THz, and 3.15 THz, 8.7 THz, respectively. The analysis of electric field and magnetic field distribution is also investigated in this paper. The effective medium ratio (EMR) for the proposed structure comes out to be 12.1 which specifies the compactness and homogeneity of the proposed metamaterial unit cell. As the proposed structure resonates in THz range, it can be employed in short-range wireless THz communication or ultrafast THz interconnects, as well as in non-destructive detection of hidden weapons.

Selection and peer-review under responsibility of the scientific committee of the International Conference on Materials, Processing & Characterization.

1. Introduction

In the last 20 years, a new form of materials called metamaterials for 3D structures and metasurfaces for 2D flat structures has been investigated. This sort of material's design flexibility provided interesting optical characteristics that drew a lot of attention and proved to be viable choices for a wide range of applications. As a result, many structures for various purposes across the electromagnetic spectrum have developed [1]. Metamaterials are extraordinarily designed electromagnetic structures whose effective permittivity and effective permeability can be changed, by adjusting the unit structure and geometric parameters which provide some unique properties like negative refractive index (NRI), electric and magnetic resonance, electromagnetic cloaking, super lenses, obstacle sensing, energy harvesting, etc [2]. Over naturally occurring materials these metamaterials show better responses for wave-matter interaction. But it all started with Victor Veselago, a Russian physicist who in 1968 introduced the world with the concept of metamaterials. He showed that these materials can have negative permittivity and permeability in a certain frequency range. In 2000, Smith [3] referred to metamaterial as Left-Handed Metamaterial (LHM) by using a combination of plasmonic-type metal wires and a split ring resonator (SRR) array to create negative electric permittivity (ε_{eff}) and negative magnetic permeability (μ_{eff}), respectively. The LHMs can be classified as DNMs (double negative metamaterial) based on both permittivity and permeability negative on particular frequency or SNMs (single negative metamaterial) based on either permittivity or permeability negative. Ordinary materials only have positive permittivity and permeability, which are known as double positive media found in nature [4].

The THz frequency ranges from 0.1 to 10 THz has numerous applications in metamaterial research which lies between the microwave and infrared region [5]. In comparison to its surrounding microwave and infrared regimes, the lack of THz materials has hampered the development of THz technology for real-world applications at terahertz frequencies, magnetic responses (permeability) can be measured using a structure made up of non-magnetic elements, such as copper-wire SRR, which show distinct responses centred around a resonant frequency. SRR have demonstrated the ability to tune in the terahertz range. It is the least studied frequency range in the electromagnetic spectrum, despite the fact that it has a wide range of uses, including secure short-range wireless communication, material characterisation, chemical

* Corresponding author.
E-mail address: mmegha848@gmail.com (Meenakshi).

https://doi.org/10.1016/j.matpr.2022.04.437
2214-7853/
Selection and peer-review under responsibility of the scientific committee of the International Conference on Materials, Processing & Characterization.

and biological spectroscopy, and sensing. THz metamaterials are discussed here, including their design, fabrication, and characterisation, with a focus on their passive and active features for THz device applications [6]. A multimode self-resonance enhanced wideband meta surface is presented in year 2021 [7]. This meta surface improves the wireless power system efficiency up to 39.2 % which was 0.04 %. With the meta surface the figure of merit (FoM) is improved to 2.09 at 90 MHz and 2.16 at 770 MHz, respectively.

A metamaterial-based absorber for terahertz based on the dielectric layer of polyimide having a H- shaped slot in the metallic plane which provides absorption peaks at 0.81 THz, 1.98 THz, 3.25 THz and 3.50 THz, respectively [8]. Tunable epsilon negative near zero index metamaterial based on symmetric resonators with high effective medium ratio for multiband wireless applications [9] offers a cross-coupled resonator-based metamaterial for satellite and RADAR communications with negative permittivity, close to zero refractive index, and an EMR of 8.03. On the other hand, a magnetically resonant meta surface with a high Q value which consist of a sandwich structure of Au film, a SiO_2 pacer layer and an Au nanorod array to enhance the Q-value. A metamaterial based on FR-4 substrate material is constructed for long range radio communications showing resonance frequencies at 2.89 GHz, 9.42 GHz and 15.16 GHz [10]. A metamaterial absorber made of tungsten film layered on silicon oxide (SiO_2) is described in another paper [11]. The absorptivity of the MTM is determined by the tungsten nanohole radius [12].A SRR on ultrathin Silicon Nitride (S_iN_x) substrate of thickness 400 nm is designed based on the planar terahertz metamaterial having resonance at 0.255 THz was detected in this SRR-MMs [13].

In this paper, a new design of leaf like metamaterial is designed for the frequency range of 1-10 μm. The scattering parameters (S_{21}) shows the two resonance frequency dips at 2.46 μm and 7.83 μm, respectively. The relative permittivity (ε_r), relative permeability (μ_r) and refractive index (η) is also evaluated. The EMR of the proposed structure comes out to be 12.1.

2. Design of the unit cell structure

The designed metamaterial is composed of copper material having thickness (t_m) 0.35 μm and conductivity (σ) 5.80 × 10^7 S/m. The FR-4 epoxy resin fibre is chosen as substrate material with dimension (L_s) 10 × 10 μm having thickness (t_s) equals to 0.8 μm with the tangent loss (δ) 0.02 and dielectric constant (ε) 4.4 as seen in Fig. 1(b). Initially on the substrate, a square ring with side dimensions of 9 μm each is built with a gap of 0.5 μm × 0.1 6 μm, two rectangles with length and breadths L_3, L_4, L_5, L_6 and eight triangles were used to create a leaf-like design inside this square ring as presented in Fig. 1(a) and dimensions of the unit cell is shown in Table 1.

3. Result and discussion

3.1. Estimation of S-parameter and electromagnetic parameters

The evaluation of scattering parameter is done in RF module Finite element method based on COMSOL Multiphysics simulation software. The electromagnetic plane wave through normal incidence is propagated along the z-axis. The Perfect Electric Conductor (PEC) and Perfect Magnetic Conductor (PMC) boundary condition is applied along the x-and y-axis with electric field polarized along y-axis. The Nicolson–Ross–Weir approach is used for the calculation of effective medium parameters i.e., permittivity (ε), permeability (μ) and refractive index (η) of the proposed structure.

The simplified formulas for the calculations are given below [14]:

$$\varepsilon_r = \frac{c}{j\pi vd}\frac{(1 - S_{11} - S_{21})}{(1 + S_{11} + S_{21})} \quad (1)$$

Table 1
Parameters with dimension of designed unit cell.

Parameters	Dimension (μm)	Description
L_1	0.5	gap width
L_2	1.6	gap height
L_3	7.0	outer rectangle length
L_4	0.3	outer rectangle breadth
L_5	2.2	inner rectangle breadth
L_6	0.4	inner rectangle length
L_7	1.6	upper triangle side
L_8	1.2	upper triangle base
L_9	2.6	lower triangle side
L_{10}	1.6	lower triangle base
L_s	10	length of substrate
L_m	9	length of material
t_s	0.8	thickness of substrate
t_m	0.35	thickness of material

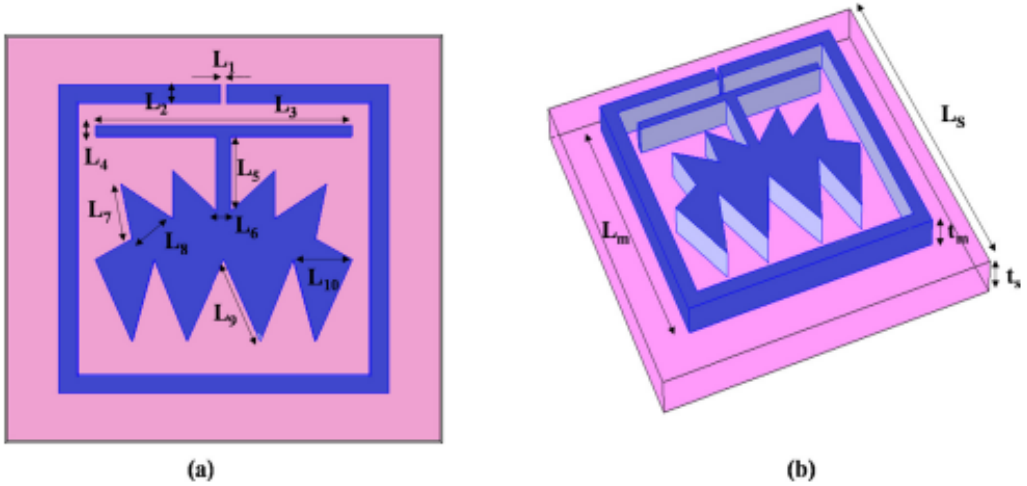

Fig. 1. (a) Front view and (b) side view of the proposed metamaterial unit cell.

$$\mu_r = \frac{c}{j\pi\nu d}\frac{(1-S_{21}+S_{11})}{(1-S_{11}+S_{21})} \quad (2)$$

$$n = \frac{c}{j\pi\nu d}\sqrt{\frac{(S_{21}-1)^2-(S_{11})^2}{(S_{21}+1)^2-(S_{11})^2}} \quad (3)$$

where, S_{11} is the reflection coefficient, S_{21} is the transmission coefficient, ν is the frequency of incident wave and d represents the thickness of the slab. The transmission coefficient (S_{21}) and reflection coefficient (S_{11}) of the proposed metamaterial unit cell are illustrated in Fig. 2.

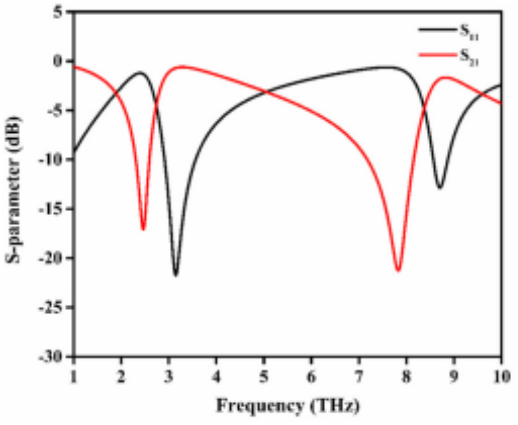

Fig 2. Scattering parameter (S_{11} & S_{21}) variation with the incident frequency wave.

The transmission coefficient (S_{21}) shows a dip at resonance frequencies 2.46 THz and 7.83 THz with the amplitudes of −17.084 dB and −21.25 dB, correspondingly, similarly the unit cell's reflection coefficient (S_{11}) showed two resonances with amplitudes of −21.74 dB and −12.865 dB at frequencies of 3.15 THz and 7.5 THz respectively. The plot of permittivity (ε), permeability (μ) and refractive index (η) of the proposed metamaterial is displayed in Fig. 3. In Fig. 3(a), the peak corresponding to frequencies 2.4 THz, 6.14 THz and 9.3 THz shows negative permittivity with amplitude −165, −684 and −300 respectively and for permeability there is slight drop on frequency for 2.4 THz as shown in Fig. 3(b) with amplitude 11.27. The negative refractive index is shown on frequencies 6 THz and 9.5 THz with amplitude −108.28 and −2 and positive refractive index on 2.79 THz with amplitude 4.8 (Fig. 3(c)).

3.2. Electric field and magnetic field distribution

The electric field and magnetic field distribution is shown in Fig. 4.

It is seen from the Fig. 4(a) that the electric field concentrates maximum in the gap (L_1) between the square ring of the order of nearly 1.82×10^7 V/m for the frequency 2.4 THz. As the frequency increases to 7.8 THz, the confinement of the electric field in the gap increases to the order of 2.8×10^7 V/m (Fig. 4(b)). With change in frequency there is a change in the electric field distribution caused by the large amount of accumulation of charges causing the meta-

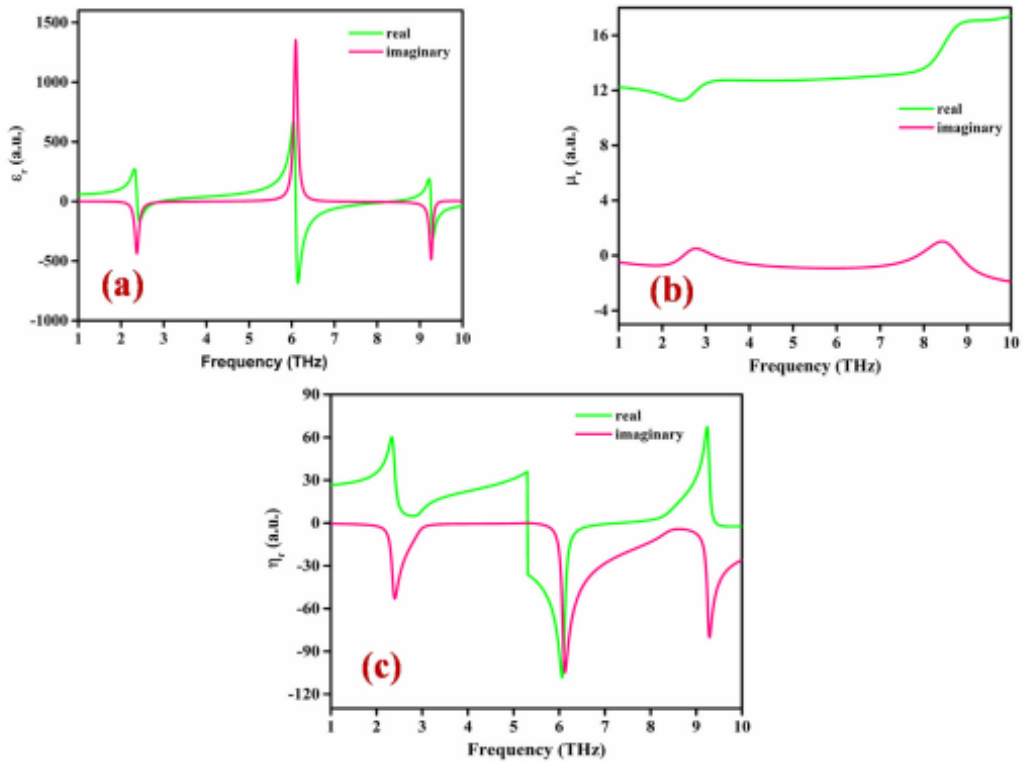

Fig 3. Variation of (a) relative permittivity (ε_r), (b) relative permeability (μ_r) and (c) relative refractive index (η) with the incident wave frequency on the proposed metamaterial unit cell.

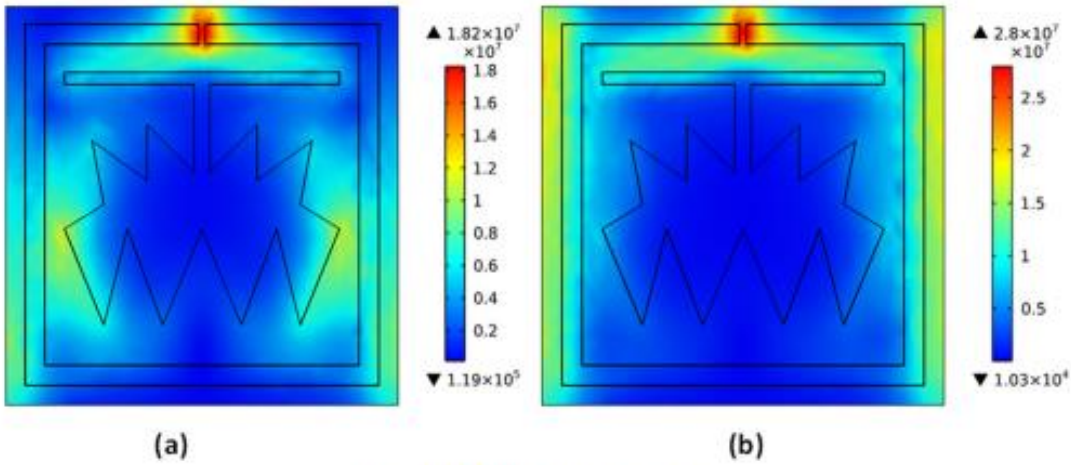

Fig 4. Electric Field at (a) 2.4 THz (b) 7.8 THz.

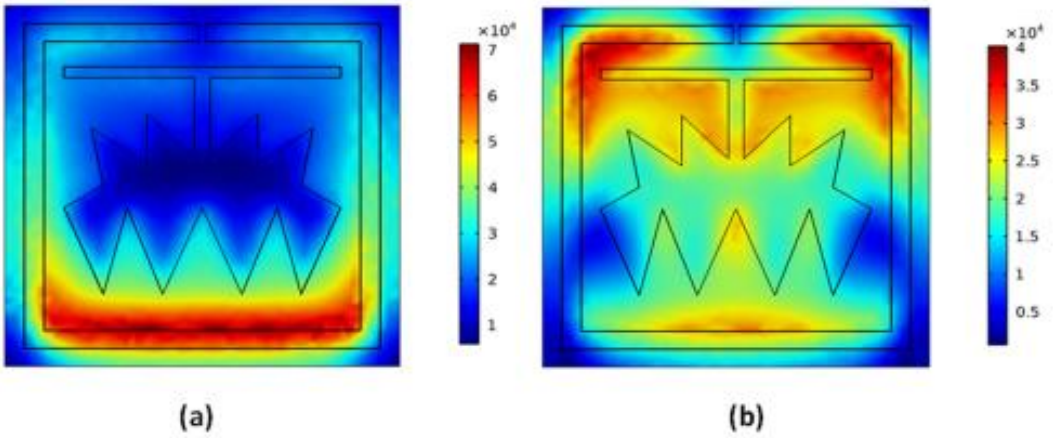

Fig 5. Magnetic Field at (a) 2.4 THz (b) 7.8 THz.

material structure to resonate in the frequency range. The plot of magnetic field distribution for the resonance frequency is presented in Fig. 5.

The magnetic field accumulate in the lower part of the structure for the resonance frequency 2.4 THz of the order of 7×10^4 A/m but for 7.8 THz the accumulation is in both upper and lower part of the structure.

3.3. Far field radiation pattern

Fig. 6 shows the Far field radiation pattern for the resonance frequenies 2.46 THz and 7.83 THz.

It is seen from the far field radiation pattern that at 2.46 THz frequency the lobe is distributed in the vertical axis showing the unidirectionality but as the frequency increases to 7.83 THz the double lobe reduces to a single lobe. The directivity of the proposed structure comes out to be 2.856 dB which shows that the designed structure can be used as antenna with the required directivity.

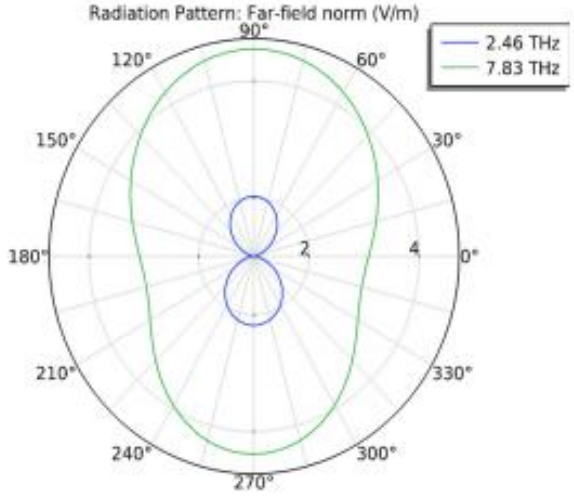

Fig. 6. Far Field radiation pattern of the designed structure.

3.4. Effective medium ratio (EMR)

The effective medium ratio (EMR) is a significant parameter for the characteristics of a metamaterial which represents the metamaterial compact size and efficiency [15]. Many devices operate at low resonance frequencies, but low resonance frequencies are difficult to accomplish due to the small size of metamaterial whereas the high EMR symbolises the perfectness and criteria fulfil

of the metamaterial design. If the EMR value is more than 4, negative permittivity is possible with the proposed metamaterial design. If the EMR value is less than 4, the metamaterial's sub wavelength condition is not met. The EMR can be calculated using a simplified formula [16]:

$$EMR = \frac{Operating\ wavelength\ of\ unit\ cell\ (\lambda)}{Unit\ cell\ length\ (L)} \quad (4)$$

The calculated value of EMR is 12.1 (10 × 10 × 1.15) for the designed metamaterial unit cell. The high value of EMR shows the compactness of the structure.

4. Conclusion

In this paper, a new leaf like metamaterial structure is designed and analyzed for THz applications in the range of 1–10 THz. The scattering parameters and propagation parameters are also evaluated. The structure resonates at two resonance frequencies i.e., 2.46 THz and 7.83 THz for transmission coefficient (S_{21}). The structure shows negative permittivity at frequency 2.46 THz. The electric and magnetic field response corresponding to the resonance frequency is also shown. Due to the small size of the suggested metamaterial unit cell, it delivers the appropriate resonance frequency and a high EMR value of 12.1.The structure can be used in the antenna with calculated value of directivity. Hence the suggested metamaterial can be effectively used in short-range wireless THz communication or ultrafast THz interconnects, as well as non-destructive detection of hidden weapons.

CRediT authorship contribution statement

Meenakshi: Conceptualization, Methodology, Data curation, Writing – original draft. **Prashant saurav:** Conceptualization, Methodology, Data curation, Writing – original draft. **Kamal Kishor:** Conceptualization, Methodology, Writing – original draft, Writing – review & editing, Supervision.

Declaration of Competing Interest

The authors declare that they have no known competing financial interests or personal relationships that could have appeared to influence the work reported in this paper.

Acknowledgments

We would like to express our heartfelt gratitude to our project supervisor, Dr. Kamal Kishor for his valuable guidance throughout the research work. We thank profusely to all the respected faculty and staff of the Department of Applied Physics, DTU for providing us the opportunity to complete our research. We also want to acknowledge our deep sense of gratitude to Mr. Ankit for his valuable time and help in the research work.

References

[1] Al-Naib, Novel terahertz metasurfaces based on complementary coupled split ring resonators, Opt. Mater. 99 (2020) 109596.
[2] A.K. Sarychev, V.M. Shalaev, Electrodynamics of metamaterials, World Scientific, 2007.
[3] D.R. Smith, J.B. Pendry, M.C. Wiltshire, Metamaterials and negative refractive index, Science 305 (5685) (2004) 788–792.
[4] M.B. Hossain, M.R.I. Faruque, S.S. Islam, M.T. Islam, Modified double dumbbell-shaped split-ring resonator-based negative permittivity metamaterial for satellite communications with high effective medium ratio, Sci. Rep. 11 (1) (2021) 1–18.
[5] M. Beruete, I. Jáuregui-López, Terahertz Sensing Based on Metasurfaces, Adv. Optical Mater. 8 (3) (2020) 1900721.
[6] M.J. Fitch, R. Osiander, Terahertz waves for communications and sensing, Johns Hopkins APL Technical Digest 25 (4) (2004) 348–355.
[7] X. Jiang, R.K. Pokharel, A. Barakat, K. Yoshitomi, A multimode metamaterial for a compact and robust dualband wireless power transfer system, Sci. Rep. 11 (1) (2021) 1–10.
[8] S.C. Bakshi, D. Mitra, L. Minz, A compact design of multiband terahertz metamaterial absorber with frequency and polarization tunability, Plasmonics 13 (6) (2018) 1843–1852.
[9] M. Moniruzzaman, M.T. Islam, I. Hossain, M.S. Soliman, M. Samsuzzaman, S.H. Almalki, Symmetric resonator based tunable epsilon negative near zero index metamaterial with high effective medium ratio for multiband wireless applications, Sci. Rep. 11 (1) (2021) 1–21.
[10] W.-Y. Tsai, C.-M. Wang, C.-F. Chen, P.C. Wu, Y.-H. Chen, T.-Y. Chen, P.R. Wu, J.-W. Chen, D.P. Tsai, Material-assisted metamaterial: a new dimension to create functional metamaterial, Sci. Rep. 7 (1) (2017) 1–6.
[11] H.u. Tao, A.C. Strikwerda, M. Liu, J.P. Mondia, E. Ekmekci, K. Fan, D.L. Kaplan, W. J. Padilla, X. Zhang, R.D. Averitt, F.G. Omenetto, Performance enhancement of terahertz metamaterials on ultrathin substrates for sensing applications, Appl. Phys. Lett. 97 (26) (2010) 261909.
[12] M. Moniruzzaman, M.T. Islam, N. Misran, M. Samsuzzaman, T. Alam, M.E. Chowdhury, Inductively tuned modified split ring resonator based quad band epsilon negative (ε) with near zero index (n) metamaterial for multiband antenna performance enhancement, Sci. Rep. 11 (1) (2021) 1–29.
[13] S.U. Afsar, M.R.I. Faruque, M.J. Hossain, M.U. Khandaker, H. Osman, S. Alamri, Modified hexagonal split ring resonator based on an epsilon-negative metamaterial for triple-band satellite communication, Micromachines 12 (8) (2021) 878.
[14] M.L. Hakim, T. Alam, A.F. Almutairi, M.F. Mansor, M.T. Islam, Polarization insensitivity characterization of dual-band perfect metamaterial absorber for k band sensing applications, Sci. Rep. 11 (1) (2021) 1–14.
[15] T. Ramachandran, M.R.I. Faruque, A.M. Siddiky, M.T. Islam, Reduction of 5g cellular network radiation in wireless mobile phone using an asymmetric square shaped passive metamaterial design, Sci. Rep. 11 (1) (2021) 1–22.
[16] A. Hossain, M.T. Islam, N. Misran, M.S. Islam, M.d. Samsuzzaman, A mutual coupled spider net-shaped triple split ring resonator-based epsilon-negative metamaterials with high effective medium ratio for quad-band microwave applications, Results Phys. 22 (2021) 103902.